

1  
2  
3  
4  
5  
6  
7  
8  
9  
10  
11  
12  
13  
14  
15  
16  
17  
18  
19  
20  
21  
22

**Comparison of TRMM 2A25 Products Version 6 and Version 7  
with NOAA/NSSL Ground Radar-based National Mosaic QPE**

Pierre-Emmanuel Kirstetter<sup>1,2,3</sup>, Y. Hong<sup>1,3</sup>, J.J. Gourley<sup>2</sup>, M. Schwaller<sup>4</sup>, W. Petersen<sup>5</sup>,  
J. Zhang<sup>2</sup>

<sup>1</sup>School of Civil Engineering and Environmental Sciences, University of Oklahoma

<sup>2</sup>NOAA/National Severe Storms Laboratory, Norman OK 73072

<sup>3</sup>Atmospheric Radar Research Center, National Weather Center, Norman OK 73072

<sup>4</sup>NASA Goddard Space Flight Center, Greenbelt, MD 20771

<sup>5</sup>NASA Wallops Flight Facility, Wallops Island, VA 23337

submitted for publication in *Journal of Hydrometeorology*

February 2012

Corresponding author:

Professor Yang Hong

National Weather Center, 120 David L. Boren Blvd,

Atmospheric Radar Research Center Suite 4610, Norman OK 73072-7303, US

e-mail: [yanghong@ou.edu](mailto:yanghong@ou.edu); <http://hydro.ou.edu>

1 Abstract

2 Characterization of the error associated to satellite rainfall estimates is a necessary  
3 component of deterministic and probabilistic frameworks involving spaceborne passive and  
4 active microwave measurements for applications ranging from water budget studies to  
5 forecasting natural hazards related to extreme rainfall events. We focus here on the error  
6 structure of Tropical Rainfall Measurement Mission (TRMM) Precipitation Radar (PR)  
7 quantitative precipitation estimation (QPE) at ground. The problem was addressed in a  
8 previous paper by comparison of 2A25 version 6 (V6) product with reference values derived  
9 from NOAA/NSSL's ground radar-based National Mosaic and QPE system (NMQ/Q2). The  
10 primary contribution of this study is to compare the new 2A25 version 7 (V7) products that  
11 were recently released as a replacement of V6. This new version is considered superior over  
12 land areas. Several aspects of the two versions are compared and quantified including  
13 rainfall rate distributions, systematic biases, and random errors. All analyses indicate V7 is  
14 an improvement over V6.

15

16 Key words: satellite-based rain estimation, radar, QPE, conditional bias, random error

17

1  
2  
3  
4  
5  
6  
7  
8  
9  
10  
11  
12  
13  
14  
15  
16  
17  
18  
19  
20  
21  
22  
23  
24  
25  
26

## 1. Introduction

Given their quasi-global coverage, satellite-based quantitative rainfall estimates are becoming widely used for hydrologic and climatic applications. Characterizing the error structure of satellite rainfall products is recognized as a major issue for the usefulness of the estimates (Yang et al. 2006; Zeweldi and Gebremichael 2009; Sapiano and Arkin 2009; Wolff and Fisher 2009) as underlined by the Program to Evaluate High Resolution Precipitation Products (Turk et al. 2008) led by the International Precipitation Working Group (IPWG; see <http://www.isac.cnr.it/~ipwg/>). In this study, we focus on the TRMM Precipitation Radar (PR) quantitative precipitation estimation (QPE) product. The TRMM-PR is currently the only active instrument dedicated to the measurement of rainfall from a satellite platform conjointly with a radiometer (TMI). PR measurements are considered as the starting point for subsequent algorithms that use microwave measurements from low-earth orbiting satellites and for combined end products that utilize data from geostationary satellites (e.g., Yang et al. 2006; Wolff and Fisher 2008, Ebert et al. 2007, Bergès et al. 2010, Ushio et al. 2006). Our aim is to compare the new PR 2A25 version 7 (V7) products that were recently released as a replacement for version 6 (V6). This new version is considered superior over land areas compared to the previous versions due to changes to the vertical profile of hydrometeor characteristics, which impacts the reflectivity-to-rainfall rate (Z-R) relationship and attenuation correction. Finally, a correction for non-uniform beam filling (NUBF) effects was reintroduced.

The methodology and framework followed here are described in a previous paper dedicated to the evaluation of 2A25 V6 (Kirstetter et al. 2012). The PR QPE product was assessed with respect to an independent reference rainfall data set derived from high-resolution measurements using NOAA/NSSL's ground radar-based National Mosaic and QPE system (NMQ/Q2; Zhang et al. 2011a). These products yield instantaneous rainfall rate

1 products over vast regions including the conterminous US (CONUS). A systematic and  
2 comprehensive evaluation for regions over the southern CONUS was performed by  
3 characterizing errors in PR estimates by matching quasi-instantaneous data from Q2 at the  
4 ~5-km pixel measurement scale of PR in order to minimize uncertainties caused by  
5 resampling. The study used three months (March-May 2011) of satellite overpasses over the  
6 lower CONUS. Despite the seemingly short period for evaluation, the use of gridded Q2 data  
7 for reference provided a large sample size totalling 392 713 comparisons. The exact same  
8 reference dataset that was used to evaluate V6 is used in this study for V7.

9 The PR and Q2 reference data are briefly described in section 2. In section 3 we assess  
10 the differences in the probability density functions (PDFs) of rain rate for 2A25 V6 and V7  
11 and their ability to represent rainfall variability. A quantitative comparison of empirical error  
12 models for V6 and V7 estimates versus reference rainfall is provided in section 4. The paper  
13 is closed with concluding remarks in section 5.

14

## 15 2. Data sources

### 16 a) Q2-based reference rainfall

17 All significant rain fields observed coincidentally by TRMM overpasses and the  
18 NEXRAD radar network from March to May 2011 are collected. The Q2 products closest in  
19 time to the TRMM satellite local overpass schedule time are used. The NOAA/NSSL  
20 National Mosaic and Quantitative Precipitation Estimation system (NMQ/Q2)  
21 (<http://nmq.ou.edu>; Zhang et al. 2011a) is a set of experimental radar-based products  
22 comprising high-resolution (0.01°, 5 min) instantaneous rainfall rate mosaics available over  
23 the CONUS (Zhang et al. 2005; Lakshmanan et al. 2007; Vasiloff et al. 2007; Kitzmiller et  
24 al. 2010). One should note that it is not possible to “validate” the PR estimates in a strict  
25 sense because independent rainfall estimates with no uncertainty do not exist. Many errors

1 affect the estimation of rainfall from ground-based radars, such as non-weather echoes,  
2 NUBF, range-dependency due to Vertical Profile of Reflectivity (VPR) variability,  
3 conversion of Z-to-R, and calibration of the radar signal. While several procedures are  
4 already in place within the Q2 system to correct for these errors, the following post-  
5 processing steps were taken to refine the reference data set as much as possible: (i) adjusting  
6 instantaneous Q2 products using co-located rain gauge observations (corrects for inaccurate  
7 Z-R relationship and calibration errors) and (ii) filtering data through a Radar Quality Index  
8 (RQI, Zhang et al. 2011b) (eliminates overestimation in the bright band and mitigates range  
9 dependency caused by VPR effects). One must keep in mind these improvements may not  
10 screen out all possible errors in ground-based radar estimates. The reference rainfall  $R_{ref}$  is  
11 a Q2 rainfall mean computed to match each PR pixel by considering the power density  
12 function of the PR beam. A standard error is computed alongside the mean reference rainfall  
13 value:  $\sigma_{footprint}$ , which represents the variability of the Q2 rainfall (at its native resolution)  
14 inside the PR footprint and is used to select the PR-Q2 reference pairs for which the  $R_{ref}$  is  
15 trustworthy (see Kirstetter et al. 2012 for more details). The reference pixels are segregated  
16 into “robust” ( $R_{ref} > \sigma_{footprint}$ ) and “non robust” ( $R_{ref} < \sigma_{footprint}$ ) estimators. Non-robust  
17 reference values are discarded for quantitative comparison. The PR rainfall statistical  
18 characteristics are preserved because the product remains free of undesirable impacts caused  
19 by resampling.

20

#### 21 *b) Precipitation Radar (PR) based rainfall*

22 The PR measures reflectivity profiles at Ku band. Surface rain rates are estimated over  
23 the southern US up to a latitude of 37°N (see Fig. 1, Kirstetter et al. 2012). The scan  
24 geometry and sampling rate of the PR lead to footprints spaced approximately 5.1 km in the

1 horizontal and along-track, over a 245-km-wide swath. The TRMM product used in this  
2 work is the PR 2A25 product (versions 6 and 7) described in Iguchi et al. (2000, 2009). The  
3 2A25 algorithm relies on a hybrid attenuation correction method that combines the surface  
4 reference technique and Hitschfeld-Bordan method (Iguchi et al. 2000; Meneghini et al.  
5 2000, 2004). Retrieval errors of the algorithm have mainly been attributed to the uncertainty  
6 of the assumed drop size distribution (DSD), incorrect physical assumptions (freezing level  
7 height, hydrometeor temperatures) and NUBF effects (Iguchi et al. 2009). Some of the  
8 weaknesses in performance with V6 (i.e., underestimation of rain-rates) over land compared  
9 to over sea previously reported (Wolff and Fisher 2008; Iguchi et al. 2009) are expected to  
10 improve as Z-R relationships over land were recalibrated and the NUBF correction, which  
11 was abandoned in V6, was re-introduced in the new V7 product.

12

### 13 **3. Rainfall data analysis**

#### 14 *a) Probability distributions by occurrence and by rain volume*

15 Hereafter, the PR rain estimates are the conditional ones (non-zero rainfall) coincident  
16 and collocated with non-zero Q2 reference estimates. In addition, the “robust” ( $R_{\text{ref}} >$   
17  $\sigma_{\text{footprint}}$ ) rain rates dataset is used as reference. Two PDFs for PR versus Q2 reference  
18 rainfall are computed and shown in Fig. 1: (i) the PDF by occurrence ( $\text{PDF}_c$ ) and (ii) the  
19 PDF by rain volume ( $\text{PDF}_v$ ) (Wolff and Fisher 2009; Amitai et al. 2009, 2011; Kirstetter et  
20 al. 2012). The  $\text{PDF}_c$  provides statistical information on the rain rate distribution and  
21 highlights the estimates’ sensitivity as a function of rain rate. The  $\text{PDF}_v$  represents the  
22 relative contribution of each rain rate bin to the total rainfall volume.

23 Compared to Q2’s reference  $\text{PDF}_c$ , both 2A25 versions tend to overestimate light rain  
24 rates ( $\sim[0.3-0.5]$  mm h<sup>-1</sup>) and demonstrate poor detection of the lightest rain rates (below  
25  $\sim 0.3$  mm h<sup>-1</sup>). A possible explanation is the edges of rain areas might be only partially

1 detected by PR because they are associated with low rain rates and intermittency (Kirstetter  
2 et al. 2012). The detectability issue is related to the sensitivity of PR and is thus not readily  
3 correctable with an update to the processing algorithm. However, it is noted that the mode of  
4 V7's  $PDF_c$  is shifted towards higher values than V6's and is more consistent with the mode  
5 of the reference  $PDF_c$ . In examining the rain rate distributions by volume, we see the modes  
6 of  $PDF_v$  for both V6 and V7 are shifted toward lower rain rates compared to the reference's  
7 mode ( $\sim 60 \text{ mm h}^{-1}$ ), which agrees with the results found in Amitai et al. (2006, 2009). This  
8 has been attributed to high rainfall rates ( $> 10 \text{ mm h}^{-1}$ ), which are likely underestimated by  
9 PR due to one or more of the following reasons: insufficient correction due to attenuation  
10 losses, NUBF effects, and inaccurate conversion from Z-to-R (Wolff and Fisher 2008). V7  
11 presents a  $PDF_v$  in better agreement with the reference than V6. The mode of the  $PDF_v$  has  
12 increased from 18 to 25  $\text{mm h}^{-1}$ , indicating a positive impact from the NUBF correction  
13 and/or Z-R improvements over land.

14

#### 15 *b) Correlations and biases*

16 Density-colored scatterplots of PR versus reference rainfall are presented for the two  
17 versions of 2A25 in Fig. 2. Improvements (i.e., increases) in V7 are evident particularly for  
18 reference rainfall values  $> 30 \text{ mm h}^{-1}$ . In addition, the underestimation from V6 at lighter  
19 rain rates ( $< 1 \text{ mm h}^{-1}$ ) has now been mitigated in V7. We also provide common comparison  
20 metrics in Table 1. A rainy pixel is included in the statistics if both PR and the reference are  
21 non-zero. The V6 and V7 estimates are both subjected to the same discrepancies in  
22 spatiotemporal matching with the Q2 reference, which is a source for differences on a point-  
23 to-point comparison basis, so their relative differences can be directly attributed to  
24 algorithms themselves. PR underestimates the mean reference rainfall values in both  
25 versions. However, the V7 products are less biased (-18%) than the prior version (-23%),

1 showing a positive impact of the new processing (i.e., recalibrated Z-R relationship over  
 2 land and NUBF correction). The correlation coefficients between both versions of PR  
 3 rainfall and Q2 reference estimates are moderate, but we note the correlation with V7 has  
 4 improved. Increasing both the bias and the correlation of the 2A25 products is a significant  
 5 achievement. In fact, it is generally recognized that it is difficult to improve one of these  
 6 statistics without the expense of the other (Ciach et al. 2000). The correction of the largely  
 7 underestimated rain rates in going from V6 to V7 (see Fig. 2) certainly contributes to this  
 8 improvement.

9

10 *c) Error models*

11 The uncertainties associated with satellite estimates of rainfall include systematic errors  
 12 as well as random effects from several sources (Yang et al. 2006; Kirstetter et al. 2011). In a  
 13 similar manner with Kirstetter et al. (2012), the departures of PR estimates from the Q2  
 14 reference values are analyzed in this section on a point-to-point basis. With the true rainfall  
 15 being unknown, the residuals are defined as the difference between the reference rainfall  
 16 ( $R_{ref}$ ) and the satellite estimates ( $R$ ):  $\varepsilon = (R - R_{ref})$ . Only pairs for which  $R_{ref}$  and  $R$  are  
 17 both nonzero are considered in the calculations. The sets of  $\varepsilon$  distributions are studied using  
 18 the generalized additive models for location, scale, and shape (GAMLSS) technique (Rigby  
 19 and Stasinopoulos 2001, 2005; Akantziliotou et al. 2002; Stasinopoulos and Rigby 2007).

20  $R_{ref}$  is considered as the main driving (explanatory) variable conditioning the departures of  
 21 PR estimates from reference values and we use the reverse Gumbel distribution

22 
$$f(\varepsilon) = \frac{1}{\sigma} \left[ -\left( \frac{\varepsilon - \mu}{\sigma} \right) - \exp \left\{ -\left( \frac{\varepsilon - \mu}{\sigma} \right) \right\} \right]$$
 to model the conditional residual distributions,

23 where the location  $\mu$  (mean of the residual population) is to be linked to systematic errors  
 24 and  $\sigma$  (the standard deviation) is representative of random errors.



1  
2  
3  
4  
5  
6  
7  
8  
9  
10  
11  
12  
13  
14  
15  
16  
17  
18  
19  
20  
21  
22  
23  
24

For a given conditional distribution of the response variable  $\epsilon$ , the conditional quantiles can be expressed as a function of  $R_{ref}$ . Figure 3 shows the residuals as a function of  $R_{ref}$  as well as the fitted GAMLSS model for the two 2A25 versions. The conditional PDFs of residuals  $\epsilon$  present a high conditional shift from the 0 line and a high conditional spread. Note that for  $R_{ref} > \sim 50 \text{ mm h}^{-1}$ , the model is quite undetermined because of the lack of observed residuals. Both 2A25 versions present a tendency to underestimate high rain rates (negative median of residuals); V6 underestimates  $R_{ref} = 20 \text{ mm h}^{-1}$  with an occurrence of 80% and with a representative bias of  $-7 \text{ mm h}^{-1}$  while V7 underestimates the same reference value with an occurrence of 75% and with a representative bias of  $-6 \text{ mm h}^{-1}$ . There is an improvement with V7, but the remaining bias is likely to be due to an inaccurate Z-R relationship, NUBF effects and/or insufficient correction of PR attenuation losses at heavier rain rates.

We consider the conditional median of the residuals to compare the systematic error component for V6 and V7 as well as the interquantile (90%-10%) value to assess the random part of the error. Figure 4 shows the conditional biases and random errors of both versions of 2A25 relative to the Q2 reference dataset. The underestimation with V6 and V7 over a large range of rain rates induces a global negative bias, which was evident in Table 1. The conditional biases of both versions relative to the reference are quite similar but with a slight improvement in V7. The random error increases consistently with  $R_{ref}$  for both products. The random part of error for V7 is greater than V6, suggesting that other factors in addition to  $R_{ref}$  could be considered to properly model the random error of V7 rain rate estimates.

**4. Conclusions**

1 A three-month dataset of gauge-adjusted, quality-filtered surface rainfall estimates from  
2 the NEXRAD-based Q2 has been used to compare and contrast PR-based 2A25 rainfall  
3 estimates from the older V6 algorithm and the newly released version (V7). V7 includes  
4 improvements in attenuation correction of the radar signal, a recalibrated Z-R equation for  
5 use over land areas, and a correction for NUBF effects was reintroduced. The comparisons  
6 have been performed at the PR-pixel resolution over the lower CONUS using a framework  
7 proposed in Kirstetter et al. (2012). Our analyses indicate that the bias of the rain rate  
8 estimates from V7 has been improved from a prior underestimation bias of -23% (from V6)  
9 to -18%. Moreover, this improvement in reducing bias is accompanied by an increase in the  
10 correlation coefficient from a prior value of 0.64 to 0.68; simultaneous improvement in both  
11 error metrics is quite challenging and was found to be a result of simultaneously correcting  
12 overestimation at lighter rain rates ( $< 10 \text{ mm hr}^{-1}$ ) and underestimation at high rain rates ( $>$   
13  $30 \text{ mm hr}^{-1}$ ). The former correction is most likely a result of the recalibration of the Z-R  
14 equation over land while the latter is likely a result from the NUBF correction; NUBF is  
15 known to cause underestimation at high rain rates (Iguchi et al. 2009).

16 A statistical error model was developed for both versions of PR algorithms to separate  
17 conditional biases and random errors as a function of reference rainfall rate. The PR  
18 residuals are confirmed to be quite large even with the newer V7 due to the aforementioned  
19 combination of error factors. Presently, the error model only considers rainfall rate of the  
20 reference as the dominant factor. A more robust error model will include the primary,  
21 identifiable error sources in PR rainfall estimates. Future work will evaluate and quantify the  
22 relative contributions of PR rainfall estimation errors linked to additional factors such as  
23 rainfall type, off-nadir angle, NUBF, attenuation, as well as influence of the underlying  
24 terrain.

25

26

1

2 *Acknowledgments*

3       We are very much indebted to the team responsible for the NMQ/Q2 products, especially  
4 Carrie Langston. This work was funded by a post-doctoral grant from the NASA Global  
5 Precipitation Measurement mission Ground Validation Management.

1 *References*

- 2 Adeyewa, Z.D., and K. Nakamura, 2003: Validation of TRMM radar rainfall data over  
3 major climatic regions in Africa. *J. Appl. Meteor.*, **42**, 331–347.
- 4 Akantziliotou, K., R.A. Rigby, and D.M. Stasinopoulos, 2002: The R implementation of  
5 Generalized Additive Models for Location, Scale and Shape. In: Stasinopoulos, M.  
6 and Touloumi, G. (eds.), *Statistical modelling in Society. Proceedings, 17th*  
7 *International Workshop on statistical modelling*, Chania, Greece, 75–83.
- 8 Amitai, E., X. Lloret, and D. Sempere-Torres, 2006: Opportunities and challenges for  
9 evaluating precipitation estimates during GPM mission. *Meteorol. Zeitschrift.*, **15**(5),  
10 551-557.
- 11 Amitai, E., X. Lloret, and D. Sempere-Torres, 2009: Comparison of TRMM Radar Rainfall  
12 Estimates with NOAA Next-Generation QPE, *Journal of the Meteorological Society*  
13 *of Japan*, **87A**, 109-118.
- 14 Amitai, E., W. Petersen, X. Lloret, and S. Vasiloff, 2011: Multi-platform comparisons of rain  
15 intensity for extreme precipitation events, *IEEE Transactions on Geoscience and*  
16 *Remote Sensing*, in press.
- 17 Berges, J.C., F. Chopin, I. Jobard, and R. Roca, 2010: EPSAT-SG: a satellite method for  
18 precipitation estimation; its concept and implementation for AMMA experiment.  
19 *Annales Geophysicae*, **28**, 289-308.
- 20 Ciach, G.J., and W.F. Krajewski, 1999: On the estimation of rainfall error variance.  
21 *Advances in Water Resources*, **2**, 585-595.
- 22 Ciach J.G., M.L. Morrissey, and W.F. Krajewski, 2000: Conditional bias in radar rainfall  
23 estimation. *Journal of Applied Meteorology*, **39**, 1941-1946.

1 Cleveland, W.S., E. Grosse, and M. Shyu, 1993: Local Regression Models. In: Chambers, J.  
2 and Hastie, T. (eds.), *Statistical Modelling in Society*, 309–376. Chapman and Hall:  
3 New York.

4 Ebert, E., 2007: Methods for verifying satellite precipitation estimates. In: *Measuring*  
5 *Precipitation from space: EURAINSAT and the future*. Levizzani, V., P. Bauer, and  
6 F.J. Turk, eds., Springer, 345-356.

7 Grimes, D.I.F., and M. Diop, 2003: Satellite-based rainfall estimation for river flow  
8 forecasting in Africa. I: Rainfall estimates and hydrological forecasts. *Hydrolog. Sci.*  
9 *J.*, **48**, 567–584.

10 Iguchi, T., T. Kozu, R. Meneghini, J. Awaka, and K. Okamoto, 2000: Rain-profiling  
11 algorithm for the TRMM precipitation radar. *J. Appl. Meteor.*, **39**, 2038–2052.

12 Iguchi, T., T. Kozu, J. Kwiatkowski, R. Meneghini, J. Awaka, and K. Okamoto, 2009:  
13 Uncertainties in the rain profiling algorithm for the TRMM Precipitation Radar. *J.*  
14 *Meteor. Soc. Japan*, **87A**, 1–30.

15 Journel, A., and C. Huijbregts, 1978: *Mining Geostatistics*. London Academic Press, 131 pp.

16 Kirstetter, P.E., G. Delrieu, B. Boudevillain, and C. Obled, 2010: Toward an error model for  
17 radar quantitative precipitation estimation in the Cévennes-Vivarais region, France.  
18 *Journal of Hydrology*, **394**(1-2), 28-41. doi:10.1016/j.jhydrol.2010.01.009

19 Kirstetter, P.E., N. Viltard, and M. Gosset, 2012: An error model for instantaneous satellite  
20 rainfall estimates: Evaluation of BRAIN-TMI over West Africa. Submitted  
21 (accepted) to *Quarterly Journal of the Royal Meteorological Society*.

22 Kirstetter, P.E., Y. Hong, J.J. Gourley, S. Chen, Z. Flamig, J. Zhang, M. Schwaller, W.  
23 Petersen, E. Amitai, 2012: Toward a Framework for Systematic Error Modeling of  
24 Spaceborne Radar with NOAA/NSSL Ground Radar-based National Mosaic QPE.  
25 Submitted (accepted) to *Journal of Hydrometeorology*.

- 1    Label, T., G. Bastin, C. Obled, and J.D. Creutin, 1987: On the Accuracy of Areal Rainfall  
2        Estimation: A Case Study. *Water Resour. Res.*, **23**(11), 2123–2134.
- 3    Label, T., C. Cappelaere, S. Galle, N. Hanan, L. Kergoat, S. Levis, B. Vieux, L. Descroix,  
4        M. Gosset, and E. Mougin, 2009: AMMA-CATCH studies in the Sahelian region of  
5        West-Africa: an overview. *Journal of Hydrology*, **375**(1-2), 3-13.  
6        doi:10.1016/j.jhydrol.2009.03.020
- 7    Lin, X., and A.Y. Hou, 2008: Evaluation of coincident passive microwave rainfall estimates  
8        using TRMM PR and ground measurements as references. *J. Appl. Meteor.*  
9        *Climatol.*, **47**, 3170–3187.
- 10   Rigby, R.A., and D.M. Stasinopoulos, 2001: The GAMLSS project: a flexible approach to  
11        statistical modelling. In: Klein, B. and Korsholm, L. (eds.), *New Trends in Statistical*  
12        *Modeling. Proceedings of the 16th International Workshop on Statistical Modelling,*  
13        Odense, Denmark, 249–256.
- 14   Rigby, R.A., and D.M. Stasinopoulos, 2005: Generalized additive models for location, scale  
15        and shape (with discussion). *Appl. Statist.*, **54**(3), pp 507-554.
- 16   Sapiano, M.R.P., and P.A. Arkin, 2009: An Intercomparison and Validation of High-  
17        Resolution Satellite Precipitation Estimates with 3-Hourly Gauge Data. *J.*  
18        *Hydrometeor.*, **10**, 149–166.
- 19   Stephens, G.L., and C.D. Kummerow, 2007: The Remote Sensing of Clouds and  
20        Precipitation from Space: A Review. *Journal of the Atmospheric Sciences* **64**(11),  
21        3742-3765.
- 22   Schumacher, C., and R.A. Houze Jr., 2000: Comparison of radar data from the TRMM  
23        satellite and Kwajalein oceanic validation site. *J. Appl. Meteor.*, **39**, 2151–2164.
- 24   Stasinopoulos, D.M., and R.A. Rigby,. 2007: Generalized additive models for location scale  
25        and shape (GAMLSS) in R. *Journal of Statistical Software*, **10**(2), 1-64.

- 1 Wolff, D.B., and B.L. Fisher, 2008: Comparisons of instantaneous TRMM ground validation  
2 and satellite rain-rate estimates at different spatial scales. *J. Appl. Meteor. Climatol.*,  
3 **47**, 2215–2237.
- 4 Takahashi, N., H. Hanado and T. Iguchi, 2006: Estimation of path-integrated attenuation and  
5 its nonuniformity from TRMM/PR range profile data. *IEEE Transactions on*  
6 *Geoscience and Remote Sensing*, **44**(11), 3276-3283.
- 7 Turk, F. J., P. Arkin, E. E. Ebert, and M. R. P. Sapiano, 2008: Evaluating high resolution  
8 precipitation products. *Bull. Amer. Meteor. Soc.*, **89**, 1911-1916.
- 9 Teo, C. K., and D.I.F. Grimes, 2008: Stochastic modelling of rainfall from satellite data.  
10 *Journal of Hydrology*, **346**(1-2), 33-50.
- 11 Ushio, T., K. Okamoto, T. Kubota, H. Hashizume, S. Shige, S. Noda, Y. Iida, K. Aonashi, T.  
12 Inoue, R. Oki, M. Kachi, N. Takahashi, T. Iguchi, 2006: A combined microwave and  
13 infrared radiometer approach for a high resolution global precipitation mapping in  
14 the GSMAP project Japan. 3rd Int. Precipitation Working Group Workshop on  
15 precipitation measurements, Melbourne, Australia.
- 16 Wolff, D.B., and B.L. Fisher, 2009: Assessing the Relative Performance of Microwave-  
17 Based Satellite Rain-Rate Retrievals Using TRMM Ground Validation Data. *Journal*  
18 *of Applied Meteorology and Climatology*, **48**(6), 1069-1099.
- 19 Yang, S., W.S. Olson, J.J. Wang, T.L. Bell, E.A. Smith, and C.D. Kummerow, 2006:  
20 Precipitation and Latent Heating Distributions from Satellite Passive Microwave  
21 Radiometry. Part II: Evaluation of Estimates Using Independent Data. *Journal of*  
22 *Applied Meteorology and Climatology*, **45**(5), 721-739.
- 23 Zeweldi, D.A., and M. Gebremichael, 2009: Sub-daily scale validation of satellite-based  
24 high-resolution rainfall products. *Atmospheric Research*, **92**(4), 427-433.  
25 doi:10.1016/j.atmosres.2009.01.001.

1 Zhang, J., K. Howard, C. Langston, S. Vasiloff, B. Kaney, A. Arthur, S. Van Cooten, K.  
2 Kelleher, D. Kitzmiller, F. Ding, D.-J. Seo, E. Wells, and C. Dempsey, 2011a:  
3 National Mosaic and multi-sensor QPE (NMQ) system: description, results and  
4 future plans. *Bull. Amer. Met. Soc.*, **92**, 1321-1338.

5 Zhang, J., Y. QI, K. Howard, C. Langston, and B. Kaney, 2011b: Radar Quality Index (RQI)  
6 – A combined measure of beam blockage and VPR effects in a national network.  
7 *Proceedings, International Symposium on Weather Radar and Hydrology*, IAHS  
8 Publ. xxx (2011).

9  
10  
11  
12  
13



1

2 **Table captions**

3

4 Table 1. Performance criteria values for PR estimates: mean, standard deviation, mean  
5 relative error (MRE) and correlation (R) with respect to references. Only the reliable Q2 data  
6 are kept (see section 2.b) for references.

7

8

1  
2  
3  
4  
5  
6  
7  
8  
9  
10  
11  
12  
13  
14  
15  
16  
17  
18  
19  
20  
21  
22  
23

**Figure captions**

Figure 1: Probability distributions of rain rates for the reference rainfall (grey) and for PR rainfall V6 (left) and V7 (right). The “robust” reference rain rates are used. The solid and dashed-dotted lines represent the distribution by volume  $PDF_v$  and the distribution by occurrence  $PDF_c$  respectively, while the grey and black lines represent the distributions for references and PR respectively. Note that the x-axis is in log-scale.

Figure 2: Scatterplots of 2A25-V6 (left) and 2A25-V7 (right) versus reference rainfall ( $mm.h^{-1}$ ). The first bisectors (solid lines) are displayed.

Figure 3: PR residuals represented versus reference (top) and the corresponding GAM model fitted and represented by [5, 10, 20, 30, 40, 50, 60, 70, 80, 90, 95] conditional quantile lines (bottom) for 2A25-V6 (left) and 2A25-V7 (right). The dotted lines represent the cumulative distribution function of the reference rainfall.

Figure 4: Conditional bias (median) of residuals (left) and conditional random error (interquantile 90%-10%) of residuals (right) for 2A25-V6 (blue) and 2A25-V7 (red) as a function of reference rainfall.

1  
2  
3  
4  
5  
6  
7  
8  
9  
10  
11

TABLE 1. Performance criteria values for PR estimates: mean, standard deviation, mean relative error (MRE) and correlation (R) with respect to references. Only the reliable Q2 data are kept (see section 2.b) for references.

<b>PR -2A25</b>	Reference	Version 6	Version 7
Mean	7.27	5.60	5.97
standard deviation	13.76	8.26	9.8
MRE / reference (%)	-	-23 %	-18 %
Correlation / reference	-	0.64	0.68

1  
2  
3  
4  
5

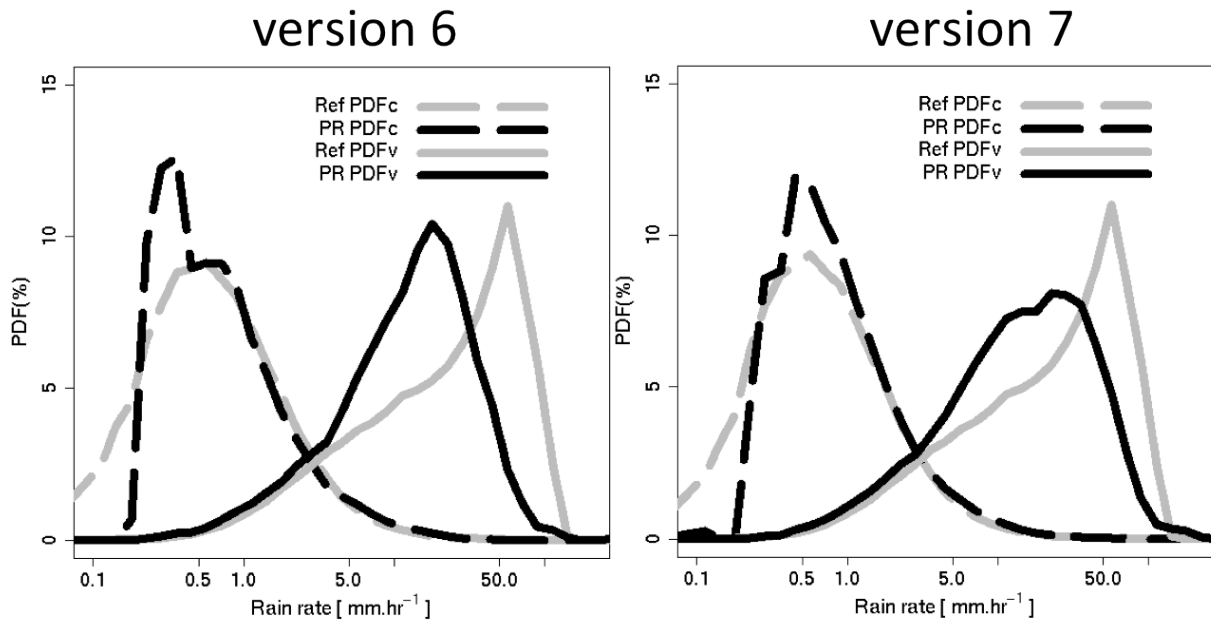


Figure 1: Probability distributions of rain rates for the reference rainfall (grey) and for PR rainfall V6 (left) and V7 (right). The “robust” reference rain rates are used. The solid and dashed-dotted lines represent the distribution by volume  $PDF_v$  and the distribution by occurrence  $PDF_c$  respectively, while the grey and black lines represent the distributions for references and PR respectively. Note that the x-axis is in log-scale.

6  
7  
8

1  
2  
3  
4  
5  
6

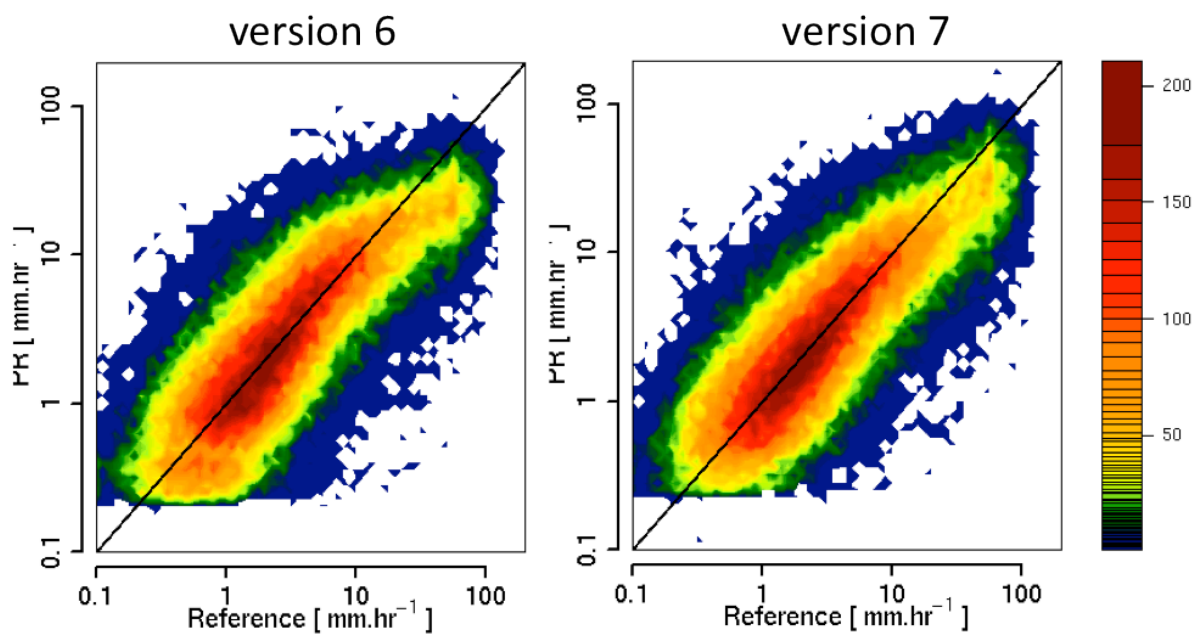


Figure 2: Scatterplots of 2A25-V6 (left) and 2A25-V7 (right) versus reference rainfall (mm.h<sup>-1</sup>). The first bisectors (solid lines) are displayed.

7  
8  
9  
10  
11  
12  
13

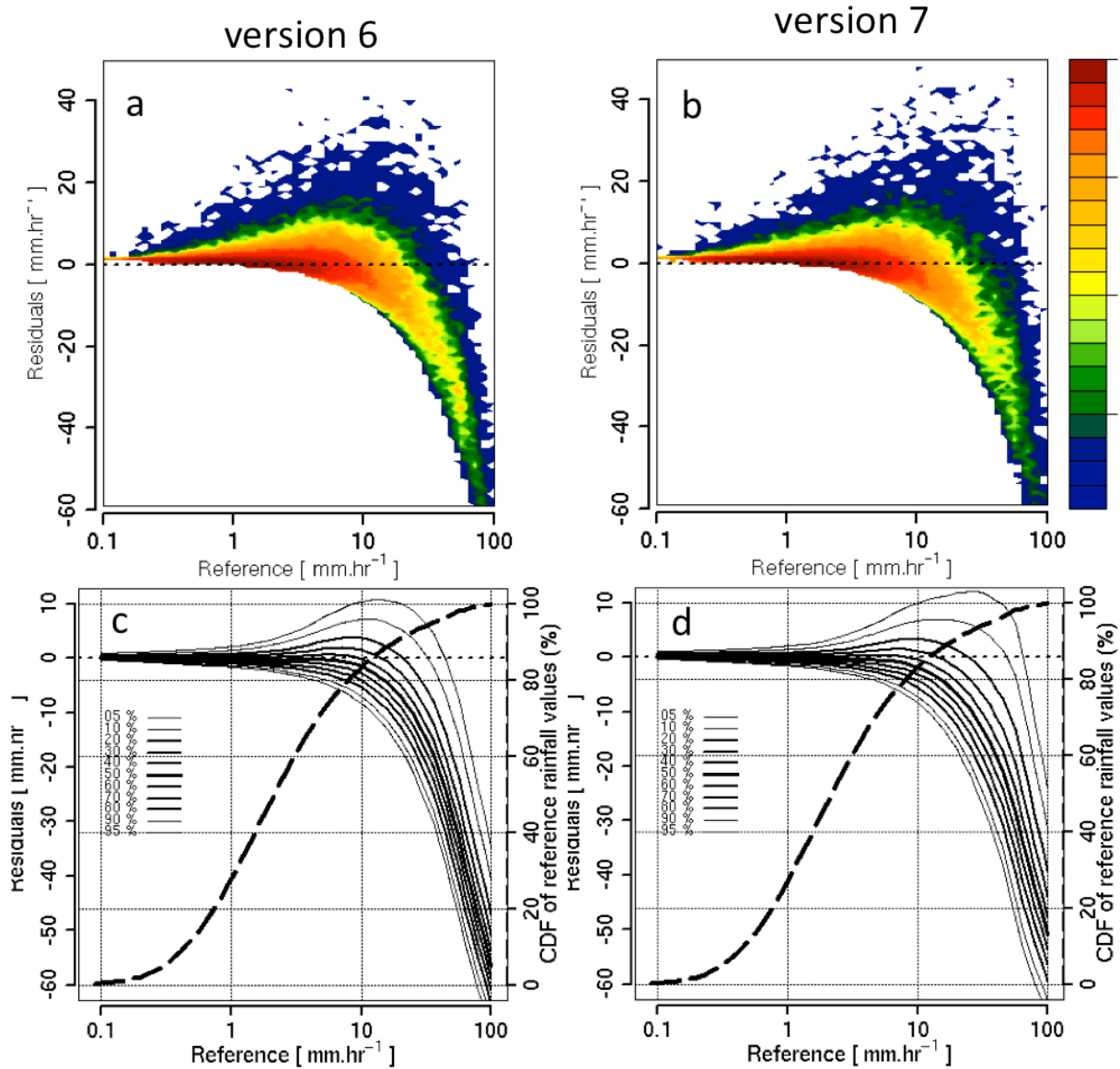


Figure 3: PR residuals represented versus reference (top) and the corresponding GAM model fitted and represented by [5, 10, 20, 30, 40, 50, 60, 70, 80, 90, 95] conditional quantile lines (bottom) for 2A25-V6 (left) and 2A25-V7 (right). The dotted lines represent the cumulative distribution function of the reference rainfall.

1  
2  
3  
4

1  
2  
3

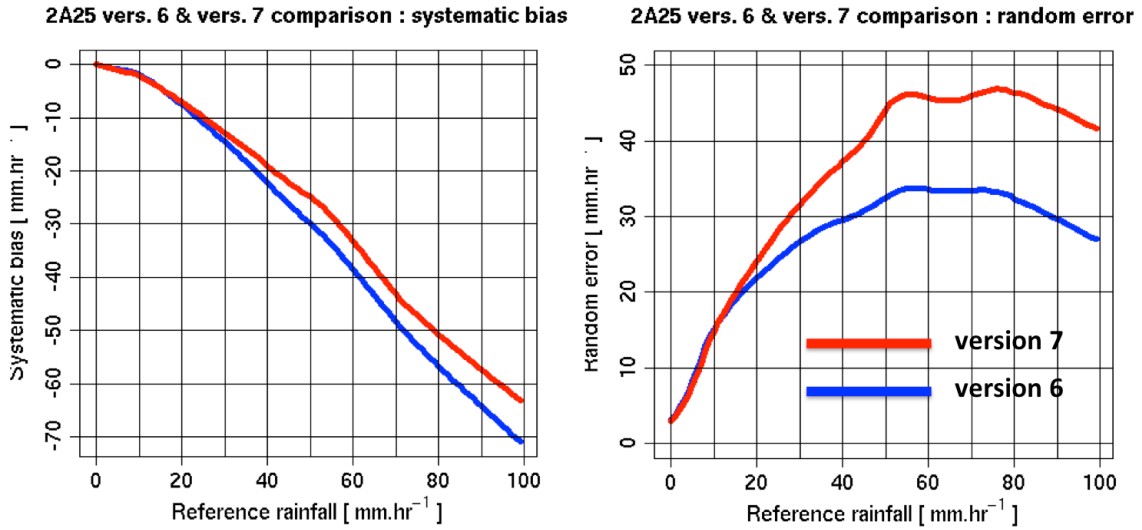


Figure 4: Conditional bias (median) of residuals (left) and conditional random error (interquantile 90%-10%) of residuals (right) for 2A25-V6 (blue) and 2A25-V7 (red) as a function of reference rainfall.

4  
5  
6